

+

# Optimising the Primary Particle Size Distributions of Pressurised Metered Dose Inhalers by Using Inkjet Spray Drying for Targeting Desired Regions of the Lungs

T. Ehtezazi<sup>1,\*</sup>, M. J. Davies<sup>1</sup>, L. Seton<sup>1</sup>, M. N. Morgan<sup>2</sup>, S. Ross<sup>2</sup>, G. D. Martin<sup>3</sup>,  
I. M. Hutchings<sup>3</sup>

<sup>1</sup> School of Pharmacy & Biomolecular Sciences, Liverpool John Moores University, Byrom Street, Liverpool, L3 3AF, UK

<sup>2</sup> General Engineering Research Institute, Liverpool John Moores University, Byrom Street, Liverpool, L3 3AF, UK

<sup>3</sup> Inkjet Research Centre, IfM, Department of Engineering, University of Cambridge, 17 Charles Babbage Road, Cambridge CB3 0FS, UK

\*Corresponding author: E-mail: [t.ehtezazi@ljmu.ac.uk](mailto:t.ehtezazi@ljmu.ac.uk), Tel: (+44)151 231 2065, Fax: (+44)

151 231 2170.

## Abstract

Conventional suspension pressurised metered dose inhalers (pMDIs) suffer not only from delivering small amounts of a drug to the lungs, but also the inhaled dose scatters all over the lung regions. This results in much less of the desired dose being delivered to regions of the lungs. This study aimed to improve the aerosol performance of suspension pMDIs by producing primary particles with narrow size distributions. Inkjet spray drying was used to produce respirable particles of salbutamol sulphate. The Next Generation Impactor (NGI) was used to determine the aerosol particle size distribution and fine particle fraction (FPF). Furthermore, oropharyngeal models were used with the NGI to compare the aerosol performances of a pMDI with monodisperse primary particles and a conventional pMDI. Monodisperse primary particles in pMDIs showed significantly narrower aerosol particle size distributions than pMDIs containing polydisperse primary particles. Monodisperse pMDIs showed aerosol deposition on a single stage of the NGI as high as  $41.75 \pm 5.76\%$ , while this was  $29.37 \pm 6.79\%$  for a polydisperse pMDI. Narrow size distribution was crucial to achieve a high FPF ( $49.31 \pm 8.16\%$ ) for primary particles greater than  $2\mu\text{m}$ . Only small polydisperse primary particles with sizes such as  $0.65 \pm 0.28\mu\text{m}$  achieved a high FPF with ( $68.94 \pm 6.22\%$ ) or without ( $53.95 \pm 4.59\%$ ) a spacer. Oropharyngeal models also indicated a narrower aerosol particle size distribution for a pMDI containing monodisperse primary particles compared to a conventional pMDI. It is concluded that, pMDIs formulated with monodisperse primary particles show higher FPFs that may target desired regions of the lungs more effectively than polydisperse pMDIs.

Key Words: Pressurised metered dose inhalers, Monodisperse particles, Spray drying, Inkjet, Oropharyngeal models

## Introduction

Monodisperse aerosol generators have been used to determine the most effective particle size of drugs such as beclomethasone dipropionate or salbutamol sulphate in the treatment of pulmonary disease.<sup>1,2</sup> A previous work suggested that 30 µg of monodisperse salbutamol sulphate aerosol particles with the aerodynamic diameter of 6 µm (inhaled from a tank) might have better bronchodilation effects than a 200 µg dose of a conventional pressurised metered dose inhaler.<sup>1</sup> The desire to favour the deposition of inhaled drug particles in the central or deep lungs was the basis of developing handheld inhalers that would produce monodisperse aerosol particles from drug solutions. In these products, the mechanisms of droplet generation were based on either electrohydrodynamic atomisation (EHDA)<sup>3</sup>, or Rayleigh jet break-up.<sup>4</sup> The EHDA based Mystic<sup>TM</sup> pulmonary drug delivery system achieved geometric standard deviation (GSD) of 1.2,<sup>5</sup> and the Rayleigh jet break-up based Medspray<sup>TM</sup> produced aerosol particles with the GSD of 1.4.<sup>4</sup> A GSD of  $\leq 1.22$  for aerosol particles has been set as a criterion for monodispersity.<sup>6,7</sup> Although the Mystic<sup>TM</sup> pulmonary drug delivery system is capable of meeting this standard, the inhaler is a relatively complex device and requires a power supply. Furthermore, the GSD of the Medspray<sup>TM</sup> has been estimated to exceed 1.22.

It should be noted that conventional inhalers have been the subject of recent investigation in the delivery of more advanced therapeutic agents to the body; here examples include monoclonal antibodies,<sup>8</sup> lung anticancer drugs<sup>9</sup> and genetic material.<sup>10</sup> A drive currently exists to develop respirable therapeutic formulations for delivery to the body in order to effectively manage a range of local and systemic disease states. We suggest that the efficacy of this route of delivery could be vastly improved if such compounds are efficiently delivered to pre-determined regions of the respiratory tract (i.e. using monodisperse particles of a

defined size). Clearly, this could optimise treatment outcomes and importantly improve patient quality of life. To reiterate, this would require knowledge of receptor sites and equivalency from one patient to another to be successful.

An alternative approach to deliver monodisperse aerosol particles to the lungs via conventional inhalers would be to incorporate ingredients with narrow particle size distributions into formulations.<sup>11,12</sup> However, previous work has served to demonstrate that in the case of conventional inhalers, in particular pressurised metered dose inhalers (pMDIs), the resulting aerosol particles may be clusters of primary drug particles.<sup>13,14</sup> Nevertheless, it is not clear whether the respirable dose would improve compared to conventional inhalers by use of monodisperse particles, and also what fraction of delivered dose might be targeted to required regions of the lungs.

To produce powders for inhalers, spray drying has been widely used.<sup>15,16</sup> However, conventional spray dryers produce particles with a wide size distribution. To overcome this, EHDA has been employed as the atomiser.<sup>17</sup> Images acquired with scanning electron microscopy suggested that the EHDA spray drying system produced particles with size distributions narrower than conventional spray drying systems.<sup>17</sup> Although in this work the GSD was not calculated, the size distribution of atomised droplets was in the range of 0-10  $\mu\text{m}$  with several droplets approximately 40  $\mu\text{m}$  in diameter. The presence of satellite droplets in an EHDA process has also been reported.<sup>18-21</sup> To scale up the throughput of EHDA based atomisers, multiple nozzle systems have been developed.<sup>22-25</sup> However, the scale-up of EHDA-based spray dryers has been impeded due to the complexity of the electrostatic field

arrangements applied to multiple jets, the specific requirements for the liquid properties and the relatively high cost to generate uniform droplets.<sup>26</sup>

An alternative approach to produce uniform droplets for spray drying is by the inkjet method. There are two common modes for generating droplets, namely the continuous mode and drop-on-demand mode.<sup>27</sup> In the continuous mode, a jet (stream) of liquid through an orifice (i.e. nozzle) is established and then with the help of a piezoelectric transducer the jet breaks-up into droplets. This process is called Rayleigh jet break-up, and if the piezoelectric transducer has a suitable frequency, then uniform droplets form.<sup>28</sup> In this mode the droplets have diameters of approximately twice that of the nozzle diameter,<sup>29</sup> and they typically travel at speeds as high as 25 m/s.<sup>30</sup> For inkjet spray drying on a laboratory scale, the droplets may therefore not have enough time to dry before reaching the collecting vessel.

With respect to the drop-on-demand mode, a piezoelectric transducer with an appropriate frequency and driving waveform generates pressure waves which eject uniform droplets from an inkjet nozzle.<sup>31</sup> In this mode, the droplets have usually the same diameter as the nozzle orifice, and also travel much more slowly. For inkjet spray drying on a laboratory scale, the droplets may therefore evaporate before reaching the cyclone or collecting vessel.

Drop-on-demand devices are normally driven at frequencies below a threshold, which is printhead dependent, where each droplet is not greatly influenced by the preceding drop. However, under some circumstances such as in our experiments, where only regular streams of droplets are required, then much higher frequencies are possible. In these cases, the size

and velocity of the drops are frequency-dependent, being influenced by the complex interactions of the acoustics and fluid flows within the printhead.<sup>32,33</sup>

An alternative method of ejecting droplets in the drop-on-demand mode is by the thermal or bubble-jet mechanism. This employs a heating element in the printhead behind the nozzle that for a short period of time increases the solution temperature, in a very thin layer close to the heater, to the range of 350-400°C.<sup>30</sup> As a result, part of the solution vaporises, generating a pressure pulse which causes droplet ejection. Although, the generation of monodisperse aerosol particles by the thermal inkjet method has been demonstrated,<sup>34</sup> the atomising head is subject to rapid degradation, due to the high temperatures.<sup>30</sup>

Inkjet spray drying based on the piezoelectric drop-on-demand mode has been previously employed for the production of uniform particles, but not for the sizes suitable for inhalation.<sup>35</sup> In this approach the viscosity and surface tension of the feed solution should be in a suitable range, to ensure formation of uniform droplets without satellites.<sup>32</sup> Furthermore, spraying suspensions should be performed carefully in terms of particle size and concentration. As drop ejection depends on receiving ultrasonic pressure waves intact to the tip of the nozzle, the presence of particles may alter the characteristics of the pressure waves and prevent droplet ejection.<sup>32</sup>

The aim of this study was to explore the feasibility of targeting desired regions of the lungs more efficiently than conventional inhalers by using pMDIs that contain monodisperse primary drug particles. In this work, piezoelectric inkjet devices were employed to produce

uniform droplets of drug solutions. The inkjet devices had orifice diameters in the range of 1  $\mu\text{m}$  to 22  $\mu\text{m}$  and the devices were operated in the drop-on-demand mode. The drug solutions were optimised to produce respirable particles in a spray drying system. Then these particles were dispersed in a propellant to form suspension-based pMDIs. The aerosol performances of pMDIs were evaluated by applying a compendial method and also the oropharyngeal models.

## **Material and Methods**

### **Material**

Salbutamol sulphate was purchased from Bufa-Chemie (Castricum, The Netherlands), polyvinylpyrrolidone (PVP K30) from Sigma and Tween 20 from VWR Ltd. Hydrofluoroalkane 134a (Zephex 134a) was kindly supplied by Ineos Fluor (Runcorn, UK). Salbutamol sulphate suspension pMDI (Ventolin™ Evohaler™ GlaxoSmithKline Ltd, London, UK, 100  $\mu\text{g}$  per actuation) was also employed. Glycerol was obtained from BDH Laboratory Supplies, and Brij35 (polyoxyethylene (23) lauryl ether) was purchased from Sigma-Aldrich (Chemie GmbH, Steinheim, Germany).

### ***Formation of Uniform Droplets***

#### ***Commercially Available Inkjet Devices***

Droplets from drug (salbutamol sulphate) and excipient (PVP K30) solutions were produced by piezoelectric inkjet devices (Microfab, Texas, USA) with 5  $\mu\text{m}$  or 10  $\mu\text{m}$  orifice diameters. To prevent blockage of the nozzles, at least two membrane filters (Minisart, Sartorius Stedim,

Germany) were used with 0.2  $\mu\text{m}$  pore size to filter the solutions prior to the inkjet devices. The devices were actuated at resonance frequencies by a frequency generator (Thurlby Thandar Instruments Ltd, Huntingdon, UK), or at 10 kHz frequency by using a Microfab frequency generator (Microfab, Texas, USA). The resonance frequencies were detected by gradual changing the frequency until sudden formation of a straight jet was observed. In all experiments double-sided square wave forms were used. Droplets were illuminated by a strobe light and visualised with a macro lens (Navitar, Rochester, New York, USA) connected to a digital USB 2.0 camera (Alrad Imaging, Newbury, UK), with an image capture rate of 60 frames per second.

#### *In-House Made Inkjet Devices*

The commercial inkjet devices were not only prone to blockage, but also very fragile. Therefore, in-house inkjet devices were manufactured from more robust glass tubes, and easy to clean. Then, the inkjet nozzles with orifice diameters of 1, 7, 14 and 22  $\mu\text{m}$  were made according to a previously reported method.<sup>36</sup> The inkjet nozzle with orifice diameter of 14  $\mu\text{m}$  was made from glass Pasteur pipette with the others from 2 mm capillary tubes. In these devices, diaphragm piezoelectric disks (Farnell, Leeds, UK) were used, and a hole at the centre of the disk was drilled to accommodate the glass tube. Conventional epoxy resin adhesives were used to hold the piezoelectric disk and glass tube together.

In order to achieve a long term stable jet, the inkjet device with 7  $\mu\text{m}$  orifice diameter had three piezoelectric disks. In this device, the first piezoelectric disk was placed at 2 mm distance from the tip of the nozzle and the other disks were attached at distances of 10 mm and 20 mm from the tip. All the three piezoelectric disks were actuated with a single function generator. However, the positive wires of the first and last (from the tip) piezoelectric disks



and the negative wire of the middle disk were connected to the positive lead of the function generator, with the reminder of the wires connected to the negative lead of the frequency generator.

The operational conditions of inkjet devices are given in Table 1. On inspection of Table 1, it is evident that satellite droplets appeared on occasions, which may be ascribed to the long term running of these devices. However, this was rapidly corrected by adjusting the frequency of the inkjet device actuation. It can be seen from Table 1 that all the experiments in this work are divided into two parts: those experiments in which there were satellite droplets during droplet formation process by the inkjet devices (formulations A to D), and those that satellite droplets were not noticed in the droplet formation process (formulations E to I). This classification is followed for the rest of the paper to make comparing the results less complex.

### ***Spray Drying System***

A laboratory scale spray dryer, Buchi 190 (BÜCHI Labortechnik AG, Switzerland) was positioned horizontally so that the top of the equipment was inside a horizontal laminar flow cabinet. A flexible tube was attached to the air inlet of the spray dryer and the other end was also placed inside the laminar flow cabinet. These arrangements ensured the entrance of clean air (dust free) into the spray dryer. The two-fluid nozzle was removed from the spray dryer and this allowed the droplets from the inkjet devices to enter the drying chamber. For the 5  $\mu\text{m}$  inkjet device, the inlet and outlet temperatures were 54 °C and 32 °C, respectively, but for the nozzles with orifices greater than this size, the inlet and outlet temperatures were

150 °C and 70 °C, respectively. The air aspiration was set to the maximum in all experiments. A high performance cyclone was used to capture the particles. Vial bottles (220 ml capacity) with 20 mm neck diameters were used as collecting vessels.

The jet was short and fine from the 1  $\mu\text{m}$  (actual orifice diameter was 1.229  $\mu\text{m}$ ) inkjet device (Figure 1). Therefore, the device was placed inside a Perspex cabinet (41  $\times$  45  $\times$  35 cm, depth, width, height, respectively) to prevent deflection of the jet by air movements around the nozzle. A 20 ml glass bottle was placed at 2 cm distance from the nozzle in a way that the jet would enter the container. Initially two solution concentrations were tested: 5% and 1% (w/v). However, crystal grains appeared inside the container when the 1% solution was used. Therefore, this concentration was not considered further. In operating the 1  $\mu\text{m}$  inkjet device, only the formation of the jet was achieved. Due to the extremely small size of droplets, it was not possible to optimise the droplet formation process.

The feed rate for the 1  $\mu\text{m}$  inkjet device was about 40 $\mu\text{l}$ /hour. For the inkjet devices with orifice diameters of 5, 7, 14, and 22  $\mu\text{m}$ , the feed rates were 0.07, 0.46, 2.0, and 2.5 ml/hour, respectively. The feed rate was 1 ml/hour for the 10  $\mu\text{m}$  inkjet device at 10 kHz frequency, but this increased to 3.5 ml/hour at the frequencies of 70 kHz and 125 kHz.

The particle collection efficiency was approximately 10% in the current spray drying system. The particle deposition efficiency was also about 10% in the container by using the 1  $\mu\text{m}$  inkjet device. This was due to the diffusion of submicron particles from the inside of the

container towards the outside. A typical density of 1.3 g/cm<sup>3</sup> was considered for produced particles.

### ***Scanning Electron Microscopy***

Spray dried particles were sputter coated with gold using an Emitech K550 (Ashford, UK) coater and then visualized with a Philips XL20 (Eindhoven, Holland) scanning electron microscope (SEM).

### ***Physical Particle Size Measurements***

The SEM images of particles were analysed for physical size measurements with the Scion Image Software, release Beta 3b (Scion Corporation, Maryland, USA). For each sample a minimum of 600 particles were analysed.

### ***Preparation of Pressurised Metered Dose Inhalers***

When the collecting vessels of the particles contained at least 20 mg of drug/excipient powder, they were crimped with the Valois (Pharmaceutical division, Normandy, France) DF30 (50- $\mu$ l metering chamber size) valves and filled with HFA 134a using a Pamasol 2016 (Pamasol, Pfäffikon, Switzerland) laboratory scale manual crimper and propellant filler. The drug concentration was in the range of 0.1-0.5 mg/g of the propellant. The bottles were shaken vigorously to detach particles from internal surfaces. The bottles were left for 3 days

at room temperature and humidity before commencing the aerosolisation studies. Due to the considerably large size of the bottles, the Qvar (IVAX Pharmaceuticals, London, UK) actuator was sliced on the canister sleeve, 9 mm above the mouthpiece. This allowed the connection of the (pMDI) valve to the nozzle of the actuator. The actuator was able to perform reciprocal movements. This actuator is referred as “actuator 1” in this paper. In other sets of experiments, another actuator was also employed that was supplied by Presspart (Blackburn, UK). This actuator had a rectangular mouthpiece with an orifice diameter (approximately 1 mm) significantly greater than that for the actuator 1. The sleeve of this actuator was detachable. This actuator is referred as “actuator 2” in this work. The inhalers were used with the actuator 1, unless otherwise stated. The aim of using different actuators was to investigate the possibility of achieving aerosol particle size distributions similar to the primary particle size distributions. The Ventolin Evohaler pMDI was used with its original actuator.

After dispersion of powder formulations from Table 1 in HFA 134a, the pMDI formulations were given the same designations as the powder formulations.

### ***Aerodynamic Particle Size Measurements***

A Next Generation Impactor (Copley, Nottingham, UK) with the USP (United States Pharmacopeia) induction port was used for aerodynamic particle size measurements. The surfaces of the impactor cups were coated with 0.5% Tween 20 solution in ethanol. The ethanol was evaporated by drying the cups in an oven. The impactor was connected to a high capacity air pump (Copley, Nottingham, UK) and air was drawn through at 30 L/min. The

test inhaler was primed by three shots to the waste and was then connected to the impactor. In addition, the effects of spacers (small and large volumes) were evaluated by using a metal large spacer (Nebuchamber, AstraZeneca, Kings Langley, UK), and a small spacer (Optimiser, Norton Healthcare Ltd, Harlow, UK). The aim of using spacers was to reduce aerosol particle aggregation in the aerosolisation experiments. The inhaler was shaken and then connected to the induction port of the impactor and while air was being drawn through the inhaler, the device was actuated, and the airflow was maintained for 8 seconds. For each aerodynamic particle size measurement the inhaler was actuated between 10 to 15 times. The impactor cups, the induction port and spacer (if used) were then washed with distilled water and the amounts of the drug were quantified by using spectrophotometric analysis at 276 nm from a standard curve. The actuator was washed with distilled water and dried in an oven before each aerosolisation experiment. The mass median aerodynamic diameter (MMAD) and GSD were calculated by plotting cumulative percentage of mass less than stated aerodynamic diameter (using log-probability scaling) versus aerodynamic diameter (log scale). The experiments were performed under ambient conditions. Each aerosolisation study was replicated six times. The fine particle fraction (FPF) was defined as the percentage of the emitted dose that had an aerodynamic diameter less than  $3.99\text{ }\mu\text{m}$ , i.e. from the stage 4 of the impactor to the minimum orifice cup (MOC). It should be noted that it was possible to fit actuator 2 only to the small spacer.

In addition, six oropharyngeal models were employed as induction ports of the NGI. The official NGI includes the USP induction port and the cups. However, in this section the USP induction port was replaced with physiologically faithful oropharyngeal (mouth-throat) models.<sup>37</sup>

The characteristics of the oropharyngeal models are given in Table 2. The models represent the oropharyngeal geometry of three subjects, each inhaling via two inhalers, one with a circular mouthpiece and the other with a rectangular mouthpiece. Models with circular inlet at the oral cavity were used to evaluate an inhaler with actuator 1. Models with rectangular inlet at the oral cavity were used to test the Ventolin Evohaler pMDI. The models varied in terms of constrictions in the oropharynx, by models 1C and 2C being constricted at the oropharynx region, models 3A and 4A were wide open, and models 5B and 6B had moderate constrictions in that region. Total volumes of the models gradually increased from model 1C to model 6B. Oropharyngeal models 1C and 2C were obtained from one subject, oropharyngeal models 3A and 4A were acquired from another subject, and finally oropharyngeal models 5B and 6B belonged to the last subject.

The models were made from ABS (acrylonitrile butadiene styrene) plastic.<sup>38</sup> The inside of each oropharyngeal model, prior to each experiment, was moisturised with a solution of glycerol and Brij 35 (70 mg in 100 ml). To achieve this, the models were filled with the solution and then they were held up right for minimum of 30 minutes to allow leaving the excess solution from the models. By this way, a thin film of the moisturising solution was formed on the internal surface of each oropharyngeal model. The airflow through the models was also set to 30 L/min. In these experiments, an inhaler (without using a spacer) was connected directly to the oropharyngeal model, and an adaptor was employed to seal the connection between the mouthpiece of the inhaler and the oral cavity. FPF was defined as the percentage of the emitted dose that deposited in the impactor. It should be noted that aerosol particles with aerodynamic diameters greater than 3.99  $\mu\text{m}$  tend to be captured by the

oropharyngeal models. Therefore, different definitions of the FPF (depending on the type of the induction port) usually specify aerosol particles with similar aerodynamic diameters. Each experiment was replicated three times when the pMDI formulation contained monodisperse particles. This was due to the availability of only limited amounts of monodisperse particles. The number of replicates was six, when the Ventolin Evohaler pMDI was used.

### ***Statistical Analysis***

The non-parametric Kruskal-Wallis tests were conducted, which followed by the two-tailed Mann-Whitney *U* tests. The Bonferroni correction was applied to the alpha level. There were 10 comparisons in total, when the formulations were evaluated by using the NGI and USP induction port. Then by applying the Bonferroni correction, the statistical significance level decreased to 0.005 (i.e. 0.05/10). In this paper SD presents the standard deviation.

## Results

### *Formation of Uniform Droplets*

Figures 2A and 2B present images of droplets being generated from the 10  $\mu\text{m}$  inkjet device at 70 and 125 kHz frequencies, respectively. Figure 2B shows a column of the solution at the tip of the nozzle, which suggests the production of droplets larger than the nozzle orifice diameter. However Figure 2A does not present that solution column at the tip, and this suggests the formation of droplets with diameters similar to the nozzle orifice diameter. The absence of solution column was also observed for inkjet devices with orifice diameters of 7, 14, and 22  $\mu\text{m}$  (images not shown). These findings indicated that the size of produced particles would also depend on the frequency of device actuation in the spray drying system.

### *Morphology and Size Distribution of Primary Particles*

Figure 3 shows SEM images of primary particles manufactured by the inkjet spray drying system. Figures 3A to 3D show non-uniformity of particle size for powder formulations A to D, respectively. While, Figures 3E to 3I illustrate formation of near uniform particles for powder formulations E to I, respectively.

The cumulative size distributions of the particles are illustrated in Figure 4A (powder formulations A to D) and Figure 4B (powder formulations E to I).

The summary of statistical parameters is given in Table 3 for the primary particle size distributions. The data suggest that the 10  $\mu\text{m}$  inkjet device produced the narrowest particle



size distribution (powder formulation I) at 10 kHz frequency (GSD of 1.05). GSDs of less than 1.22 were also found for powder formulations E, G, and H (Table 3). However, the GSD was above 1.22 when there were satellite droplets in the droplet formation process (powder formulations A to D), or actuating the inkjet device at 125 kHz (powder formulation F). The aim of actuating the inkjet device at 125 kHz was to increase the powder production throughput compared to actuating the inkjet device at 70 kHz. However, limited benefit was noted at these particular occasions. As the solution feed rate remained relatively unchanged (3.5 ml/ hour) and also GSD increased by increasing the frequency.

### ***Physical Stability of pMDI Formulations***

The prepared formulations did not show signs of sedimentation for up to two months after preparation when the primary particles were prepared by the commercial inkjet devices (pMDI formulations B, E, F, H, I). Figure 5A presents a typical example of these formulations three days after preparation. However, the formulations did show precipitation within 24 hours after preparation (Figure 5B) when the primary particles were made by the in-house inkjet devices (pMDI formulations A, C, D, G). It should be noted that the commercial inkjet devices had metal guards at the tip of the nozzle (indicated in Figure 2). Therefore, the variation in designs of inkjet devices might have affected on the physical properties of the particles and consequently on the physical stability of pMDI formulations. It appears that the aerosol performances of pMDI formulations were affected by the state of the physical stability of the pMDI formulations (data presented in the following section).

## ***Aerodynamic Particle Size Distributions***

### *Evaluations with the USP Induction Port*

Figures 6A and 6B present the aerodynamic particle size distributions of the pMDI formulations within the impactor when a spacer was used, while Figure 6C shows the aerosol particle size distributions when the inhalers were used without a spacer. Table 3 shows the summary of the cascade impaction data.

### *The Effects of Spacer Devices*

Formulations E, G, H and I had primary particles with a GSD less than 1.22. These showed low aerodynamic GSDs (i.e. ranging from  $1.43 \pm 0.10$  to  $1.63 \pm 0.04$ ), when these pMDIs were tested with the large spacer and actuator 1 (Table 3). Conversely, pMDI formulations A to D contained polydisperse primary particles and they showed relatively greater aerodynamic GSDs (i.e. ranging from  $1.59 \pm 0.10$  to  $3.32 \pm 0.37$ ), when these formulations were evaluated with the large spacer and actuator 1. Increasing the PVP proportion in the primary particles (powder formulations A to D, F and G in Table 1) did not make the aerodynamic GSD (pMDI formulations A to D, F and G) similar to the GSD of primary particles (Table 3).

Figure 6B shows that pMDI formulations E to I (contained near monodisperse primary particles) had aerosol depositions in the range of  $36.38 \pm 2.50\%$  to  $41.75 \pm 5.76\%$  (of the emitted dose) on a single impactor stage. While among pMDIs that contained polydisperse primary particles, maximum deposition on a single stage was  $29.24 \pm 4.2\%$  (pMDI formulation B, stage 4, Figure 6A). These formulations were evaluated with the large spacer

and actuator 1. Here a similar trend was also observed for pMDI formulations C and G, when these were evaluated with actuator 1 but without a spacer (Figure 6C). Formulation G showed significantly ( $P=0.002$ ) higher aerosol deposition ( $27.77 \pm 5.04\%$ ) on the stage 4 than pMDI formulation C on the same stage ( $10.80 \pm 1.07\%$ ).

The results presented in Table 3 indicate that the FPF of pMDI formulation F ( $66.29 \pm 5.46\%$ ) was greater than that for pMDI formulation C ( $54.92 \pm 3.83\%$ ), when these were evaluated with the large spacer and actuator 1. Although the difference did not reach the significance level ( $P=0.015$ ). Furthermore, Figure 6B confirms that pMDI formulation F had  $37.35 \pm 2.76\%$  of the emitted dose depositing on the stage 4, while this was  $17.37 \pm 2.16\%$  for pMDI formulation C (Figure 6A), when these formulations were evaluated with the large spacer and actuator 1. These differences were despite of similarity of primary particles of pMDI formulation C and pMDI formulation F in terms of size ( $1.59 \pm 0.38 \mu\text{m}$  and  $2.03 \pm 0.43 \mu\text{m}$ , respectively) and GSD (1.25 and 1.26, respectively). Those dissimilarities in aerosol performances might be explained by the improved physical stability of pMDI formulation F compared to pMDI formulation C.

The data in Figure 6B indicate that pMDI formulations E to H could be suitable for targeting the medium sized airways, while pMDI formulation I could target mainly the large conducting airways.

### *The Effects of Primary Particle Size Distribution (Polydisperse vs Monodisperse)*

It is apparent from Table 3 that pMDI formulation D had similar average primary particle size ( $2.39\ \mu\text{m}$ ) as powder formulation G ( $2.36\ \mu\text{m}$ ) and powder formulation H ( $2.65\ \mu\text{m}$ ), but the primary particle size distribution in pMDI formulation D was wider (GSD of 1.45) than those for pMDI formulation G (GSD of 1.14) and pMDI formulation H (GSD of 1.14).

Evaluating these pMDI formulations with the large spacer and actuator 1 indicated that drug deposition in the spacer was much higher for pMDI formulation D ( $48.67 \pm 5.20\%$ ) than those for pMDI formulation G ( $21.98 \pm 16.84\%$ ) and pMDI formulation H ( $25.22 \pm 7.43\%$ ) (Figures 6A and 6B). Furthermore, pMDI formulation G had significantly greater FPF ( $59.18 \pm 12.73\%$ , Table 3), smaller MMAD ( $2.05 \pm 0.20\ \mu\text{m}$ ) and aerodynamic GSD ( $1.63 \pm 0.04$ ) compared to pMDI formulation D ( $27.32 \pm 1.70\%$ ,  $3.22 \pm 0.50\ \mu\text{m}$ ,  $2.48 \pm 0.70$ , respectively) ( $P=0.002$ ). Likewise, pMDI formulation H had significantly greater FPF ( $46.67 \pm 2.06\%$ ) and smaller aerodynamic GSD ( $1.48 \pm 0.11$ ) than those for pMDI formulation D ( $P=0.002$ ). These observations indicate that pMDI formulations with monodisperse primary particles would have significantly higher FPFs and smaller aerodynamic GSDs than those for pMDI formulations with polydisperse primary particles. In particular, when the primary particles are in the range of  $2.36 \pm 0.34\ \mu\text{m}$  to  $2.65 \pm 0.34\ \mu\text{m}$ .

Table 3 indicates that pMDI formulations A, B, E and F achieved FPFs greater than 60%, when these were examined with the large spacer and actuator 1. Primary particles gradually increased in size from  $0.65 \pm 0.28\ \mu\text{m}$  to  $2.03 \pm 0.43\ \mu\text{m}$  in the order of pMDI formulation  $A < B < E < F$ , but FPFs remained relatively unchanged. For example, the FPF of pMDI formulation A ( $68.94 \pm 6.22\%$ ) was not statistically different ( $P=0.589$ ) from FPF of pMDI formulation F ( $66.29 \pm 5.46\%$ ). Interestingly, the GSD of primary particles decreased from

1.60 to 1.07 in the order of pMDI formulation A<B<F<E. These observations indicate that if pMDI formulations contain polydisperse primary particles, then these formulations may achieve high FPFs if average primary particle size becomes close to 1.15  $\mu\text{m}$  or even 0.65  $\mu\text{m}$ .

#### *The Aerosol Performance of Submicron Primary Particles*

Table 3 shows that pMDI formulation A had MMADs considerably greater than the size of primary particles ( $0.65 \pm 0.28 \mu\text{m}$ ) with or without using the large spacer ( $2.20 \pm 0.36 \mu\text{m}$ , and  $2.30 \pm 0.43 \mu\text{m}$ , respectively). Furthermore, Figure 6A shows that the drug deposition ( $27.51 \pm 4.81\%$ ) was the highest on the stage 5 (cut off diameter 1.36  $\mu\text{m}$ ) for this formulation. These observations suggest that most of aerosol particles were made of clusters of small primary particles. Then this aggregated nature of aerosol particles contained considerable amount of void space. Therefore, the FPF of pMDI formulation A with the large spacer ( $68.94 \pm 6.22\%$ ) or without a spacer ( $53.95 \pm 4.59\%$ , Table 3) became significantly greater than those for a conventional pMDI such as the Ventolin with the large spacer ( $57.32 \pm 1.31\%$ ,  $P=0.004$ ) or without a spacer ( $33.48 \pm 1.91\%$ ,  $P=0.002$ ).

#### *Comparison of Actuators*

Figures 6A and 6C show that aerosol depositions reduced considerably on impactor stage 1, stage 2, and stages 6 to MOC by using actuator 2 for pMDI formulation C, compared to aerosol depositions on those stages by using the actuator 1. As a result the GSDs of aerosol particles from pMDI formulation C used with actuator 2 were smaller than those for pMDI formulation C used with actuator 1 (Table 3). However, actuator 2 also reduced considerably

FPFs, compared to those FPFs by using actuator 1 (Table 3). These findings show that the type of actuator had paramount effects on the aerosol performances of pMDIs.

#### *Evaluations with the Oropharyngeal Models*

Figure 7A presents aerosol depositions in the impactor by using the oropharyngeal models (2C, 4A, 5B) for pMDI formulation G (containing monodisperse primary particles with diameter of  $2.36 \pm 0.34 \mu\text{m}$ ). Upon inspection of Figure 7A, it is evident that stage 4 showed maximum drug deposition, as formulation G showed with the USP induction port (Figure 6C). Figure 7A also shows that the amount of drug deposited on the stage 4 increased by increasing the oropharyngeal volume. The drug deposition on the stage 4 was  $5.91 \pm 4.84\%$  of the emitted dose. However, the drug deposition was spread mostly from the stage 4 to stage 6 for a conventional polydisperse pMDI such as the Ventolin (Figure 7B). The stage 5 showed maximum aerosol deposition ( $3.13 \pm 1.65\%$  of the emitted dose).

The summary of cascade impaction data for the oropharyngeal models is given in Table 4. Data in Table 4 show that the aerodynamic GSDs of pMDI formulation G were smaller (ranging from  $1.18 \pm 0.11$  to  $1.28 \pm 0.03$ ) than the aerodynamic GSD of this formulation when it was evaluated with the USP induction port but without a spacer ( $2.36 \pm 0.64$ , Table 3). Furthermore, pMDI formulation G showed GSDs considerably smaller than the GSDs of the Ventolin (ranging from  $2.37 \pm 0.19$  to  $2.81 \pm 0.26$ ), when these formulations were examined with the oropharyngeal models (Table 4). However, the average FPF ( $9.88 \pm 6.10\%$ ) of all three oropharyngeal models for pMDI formulation G was comparable to the average FPF ( $9.60 \pm 4.58\%$ ) of all three oropharyngeal models for the Ventolin. These

observations suggest that pMDIs with monodisperse primary particles may target desired regions of the lungs more effectively than pMDIs with polydisperse primary particles.

### ***Morphology and Size of Primary Particles After Dispersion in HFA***

Aerosol depositions (about 10% of the emitted dose) were not expected on the MOC stage (cut off diameter less than 0.54  $\mu\text{m}$ ) of the impactor from pMDI formulation G (Figures 6B, 6C, 7A). This expectation was based on the fact that all of primary particles being greater than 1  $\mu\text{m}$ . To investigate further, the HFA was evaporated from pMDI formulation G, and then the residual powder was examined by SEM. It was found that the primary particles of pMDI formulation G had particle size of  $2.39 \pm 0.32 \mu\text{m}$  with the GSD of 1.14 after dispersion in HFA 134a. These particles had sizes similar to the primary particles of pMDI formulation G before dispersion in the propellant ( $2.36 \pm 0.34 \mu\text{m}$ , GSD of 1.14, Table 3). Figure 8 compares SEM images of primary particles of pMDI formulation G before and after dispersion in HFA 134a. It can be seen that physical diameters and the surface morphology of the primary particles remained relatively unchanged after dispersion in HFA 134a. By considering that only 10% of primary particles had a size in the range of 1.8  $\mu\text{m}$  to 2.07  $\mu\text{m}$ , then the aerosol deposition on the MOC stage could be due to these primary particles.

## **Discussion**

This study showed that primary particle size and particle size distribution had significant effects on the aerosol performances of suspension pMDIs, and indeed inkjet spray drying may be useful in producing primary particles with a desired size.

This study suggests that to achieve a pMDI with relatively high FPF then for primary particles in the range of 1.59  $\mu\text{m}$  to 2.03  $\mu\text{m}$ , the GSD should be less than 1.25, and for primary particles greater than 2.03  $\mu\text{m}$ , the GSD should be less than 1.14. If the desired GSD of primary particles is approximately 1.45, then the sizes of these particles should be in the region of 1.15  $\mu\text{m}$ .

This study found that pMDIs with monodisperse drug particles had increased fine particle fractions and also narrower aerodynamic particle size distributions compared to a formulation with similar average primary particle size but being polydisperse. The aerodynamic GSDs of pMDI formulations prepared with monodisperse particles were greater than the GSDs of the primary particles. Perhaps this would be expected by considering the polydisperse nature of propellant droplets generated during aerosolisation.<sup>13,14</sup> However, the monodisperse pMDIs delivered up to 40% of the emitted dose to a single stage of the NGI when the USP induction port, a large volume spacer and an actuator with 0.3 mm orifice diameter were used.

Previous studies<sup>39,40</sup> showed much narrower aerosol particle size distributions for pMDIs containing 5  $\mu\text{m}$  polystyrene particles than the pMDI in this study that contained 4.99  $\mu\text{m}$  monodisperse salbutamol sulphate particles. Then a smaller GSD might have been achieved in this study, if the formulation would have been optimised further in terms of surfactant type, valve size and the volume of spacer.

It should be noted that asthma is a highly complex disease. Only recent studies have shown distinct asthma phenotypes, which may require distinct therapeutic approaches and agents.<sup>41</sup>



If the chosen therapeutic agent has significant side effects, then a monodisperse inhaler could benefit the patient by reducing the dose of inhaled drug required to obtain the equivalent clinical outcome.<sup>41</sup>

The respirable doses determined by the oropharyngeal models in this study were similar to clinical data determined for the Ventolin Evohaler,<sup>42</sup> and these were less than those determined by using the USP induction port with the cascade impactor. Also, the respirable doses of the oropharyngeal models were less than those for the USP induction port for a pMDI containing monodisperse primary particles. However, the results of this study found that certain subjects (those with large volume oropharynx and moderately constricted during inhalation) could receive considerably more respirable doses by using pMDIs containing monodisperse particles than conventional pMDIs. For other subjects, the amounts of respirable doses may not increase by using pMDIs containing monodisperse particles, but the deposition of aerosol particles could be accumulated in certain and perhaps desired regions of the lungs.

The aerosol particle size distribution data for a pMDI formulation that contained submicron primary particles suggested that the use of submicron particles may not be the solution to target the alveoli by suspension pMDIs. The results of this study suggested that primary particles with physical diameters in the range of 1.8  $\mu\text{m}$  to 2  $\mu\text{m}$  with extensively corrugated surfaces may target peripheral lungs or alveoli by using suspension pMDIs.

In this study a single inkjet device was used for spray drying, while for production at an industrial scale or even for small batch sizes at the pilot scale, a multi-nozzle system would be required. To achieve a multi-nozzle system for inkjet spray drying, micro-nozzle plates<sup>43</sup> or droplet-ejector nozzle arrays<sup>44,45</sup> could be potential starting points. Then existence of these systems would allow producing powders with a sufficient amount to evaluate the effects of particle size uniformity on powder properties such as powder flow.

The particles manufactured in this study had narrower size distributions than the results of Patel and Chen 2007.<sup>35</sup> This could be due to differences in the orifice diameters of the inkjet nozzles. The orifice diameter of the nozzle in the previous study was 80  $\mu\text{m}$ , whereas in this study they were in fact smaller. Therefore, the narrower particle size distributions could be explained by the fact that the droplets from smaller nozzles were dried faster than droplets from the larger size nozzle. This would provide less time and thus opportunity for the droplets to merge. Increasing the drying chamber size and scattering droplets with the help of an air diffuser resulted in the production of monodisperse particles from a 75  $\mu\text{m}$  orifice diameter inkjet device.<sup>46</sup>

The formulations developed in this study did not contain ethanol to disperse the particles. Also, relatively large amounts of propellant were introduced into the pMDI bottles. Therefore, further studies are required to determine whether the presence of ethanol or increasing the formulation solid content would influence on the aerosol performances of the inhalers.<sup>47,48</sup>

Part of inhalers in this study showed a significant improvement in physical stability compared to those reported previously.<sup>49</sup> This might be explained by the presence of electrostatic charges on the particles. This explanation may be supported by the fact that the inkjet method allows charging of the ejected droplets. This is frequently applied in the printing industry, when the mode of droplet formation is the continuous mode.<sup>27</sup> We propose that an avenue for further study would involve preparing monodisperse particles with different levels of electrostatic charges and using these in formulations of suspension pMDIs. This step would be followed by measuring the electrostatic charge of aerosol particles by previously reported methods<sup>50</sup> and evaluating physical stability together with the aerosol performance.

Aerodynamic particle size analysis plays a key role for manufacturers not only for quality control purposes, but also to maintain the efficacy of the product. Therefore, less batch-to-batch variation could be another expectation of using uniform primary particles in the manufacture of orally inhaled suspension drug products. In particular, this may lead to achieving reproducible measurements of aerodynamic particle size distributions using cascade impactors, batch after batch.<sup>51</sup> In addition, the use of monodisperse particles at industrial scale would aid in understanding and optimisation of the manufacturing process. Therefore, the use of monodisperse particles may help better implementation of the quality by design (QbD). Also, the use of monodisperse particles would reduce variation in the raw material, which would ensure that quality is built into pharmaceutical products.<sup>52</sup> Furthermore, the ability to produce monodisperse primary particles in an industrial scale and using them in the formulation of an inhaler may provide unique properties to the product that could be challenging for competitors to match the product after the product is off the patents.

In this work an inkjet device was used that had triple piezoelectric components and the orifice diameter was 7  $\mu\text{m}$ . This device showed much improved jet stability over a long term run compared to a device with single piezoelectric component and similar orifice diameter. This observation might be explained that in the triple disk inkjet device the negative pressures were much stronger than those in the single piezoelectric inkjet device.<sup>32</sup> Therefore, if small particles in the feed solution were about to interfere with the droplet formation process, then (in the triple disk inkjet device) they were removed with a strong force away from the nozzle orifice.

## Conclusions

This study demonstrated significant improvement in the fine particle fraction (FPF) of pressurised metered dose inhalers (pMDIs) that contained monodisperse primary particles compared to FPF of pMDIs that contained similar average primary particle size but being polydisperse. Furthermore, pMDIs with monodisperse primary particles may target regions of the lungs more effectively than conventional inhalers.

This study found that to achieve a high FPF, for primary particles with average size in the range of 0.65  $\mu\text{m}$  to 1.15  $\mu\text{m}$  the GSD could be high in the range of 1.45 to 1.60. While for primary particles with average size in the range of 1.5  $\mu\text{m}$  to 2  $\mu\text{m}$ , the GSD should be less than 1.25; and for primary particles greater than 2  $\mu\text{m}$ , the GSD should be less than 1.14. An actuator with orifice diameter of 0.3 mm played an important role for delivery of high FPFs.

The results of this study suggest that the inkjet spray drying may be used to achieve primary particles with precise size. Furthermore, the inkjet method may provide additional optimisation of particles and then achieving suspension pMDIs with significantly improved physical stability.

## **Acknowledgement**

The authors would like to thank Valois (France) for providing valves, Presspart (Blackburn, UK) for supplying actuator, and Microfab (Texas, USA) for technical assistance.

## List of Figures

**Figure 1.** A photograph of the 1  $\mu\text{m}$  inkjet device while emitting droplets. The piezoelectric disk and tip of the nozzle are indicated.

**Figure 2.** Stroboscopic images of droplet formation via the 10  $\mu\text{m}$  inkjet device at frequencies: A) 70 kHz, B) 125 kHz. The metal guard is shown and the formation of fluid column at the tip of the nozzle is also indicated.

**Figure 3.** Panels A to D, SEM images of particles for powder formulations A to D, which contained polydisperse particles. Panels E to I, SEM images of particles for powder formulations E to I, which contained near-uniform particles.

**Figure 4.** A) Cumulative under size distributions for powder formulations A to D that contained polydisperse particles. B) Cumulative under size distributions for powder formulations E to I that contained near-uniform particles.

**Figure 5.** A) Presenting physical stability of a pMDI that the primary particles were prepared by the 10  $\mu\text{m}$  inkjet device, which had metal guards. This picture was taken three days after preparation of the pMDI. B) Illustrating the sedimentation of the primary particles the next day after preparation, in a pMDI that the primary particles were produced by an in-house inkjet device. The primary particles were made by the 7  $\mu\text{m}$  inkjet device, which did not have metal guards.

**Figure 6.** Drug deposition distributions of pMDI formulations in the Next Generation Impactor with the USP induction port. A) Using a spacer, pMDI formulations contained polydisperse primary particles. B) Using a spacer, pMDI formulations contained near monodisperse primary particles. C) Formulations were evaluated without a spacer. Error bars present standard deviations ( $n=6$ ).

**Figure 7.** A) Drug deposition distributions of pMDI formulation G (prepared with monodisperse primary particles) in the Next Generation Impactor with the oropharyngeal models: 2C, 4A and 5B. B) Drug deposition distributions of the Ventolin in the Next Generation Impactor with the oropharyngeal models: 1C, 3A, and 6B. Error bars present standard deviations. Data labels are also indicated. The *key to symbols* also shows the corresponding oropharyngeal volume.

**Figure 8.** The SEM images of primary particles of pMDI formulation G (prepared with monodisperse primary particles), A) before and B) after dispersion in HFA 134a.

## References

1. Usmani OS, Biddiscombe MF, Barnes PJ. Regional lung deposition and bronchodilator response as a function of beta2-agonist particle size. *Am J Respir Crit Care Med* 2005;172:1497-1504.
2. Esposito-Festen JE, Zanen P, Tiddens HA, Lammers JW. Pharmacokinetics of inhaled monodisperse beclomethasone as a function of particle size. *Br J Clin Pharmacol* 2007;64:328-334.
3. Zimlich WC, Ding JW, Busick DR, Moutvic RR, Placke ME, Hirst P, Pitcairn GR, Malik S, Newman SP, Macintyre F, *et al.* The development of a novel electrohydrodynamic (EHD) pulmonary drug delivery device. In: Dalby RN, Byron PR, Farr SJ, Peart J, editors. *Respiratory drug delivery VII. Volume 1*. Raleigh, NC: Serentec Press; 2000. pp. 241–246.
4. de Boer AH, Wissink J, Hagedoorn P, Heskamp I, de Kruijf W, Bunder R, Zanen P, Munnik P, van Rijn C, Frijlink HW. In vitro performance testing of the novel Medspray wet aerosol inhaler based on the principle of Rayleigh break-up. *Pharm Res* 2008;25:1186-1192.
5. Zimlich WC, Ding JW, Busick DR, Pham S, Palmer D, , Placke ME. Development of multiple clinical and commercial applications using Mystic inhalation delivery technologies. In: Dalby RN, Byron PR, Peart J, Farr SJ, editors. *Respiratory drug delivery VIII. Volume 2*. Raleigh, NC: Davis Horwood; 2002. pp. 363–366.
6. Morrow, P.E., 1981. An evaluation of the physical properties of monodisperse and heterodisperse aerosols used in the assessment of bronchial function. *Chest* 80, 809–812.
7. Biddiscombe MF, Usmani OS, Barnes PJ. A system for the production and delivery of monodisperse salbutamol aerosols to the lungs. *Int J Pharm* 2003;254:243-253.
8. Hacha, J., Tomlinson, K., Maertens, L., Paulissen, G., Rocks, N., Foidart, J.M., Noel, A., Palframan, R., Gueders, M., Cataldo, D.D. Nebulized anti-IL-13 monoclonal antibody Fab' fragment reduces allergen-induced asthma. *Am J Respir Cell Mol Bio* 2012, 47:709-717.
9. Lemarie, E., Vecellio, L., Hureauux, J., Prunier, C., Valat, C., Grimbert, D., Boidron-Celle, M., Giraudeau, B., le Pape, A., Pichon, E., Diot, P., el Houfia, A., Gagnadoux, F. Aerosolized gemcitabine in patients with carcinoma of the lung: feasibility and safety study. *J Aerosol Med Pulm Drug Deliv* 2011; 24:261-270.
10. Conti, D.S., Bharatwaj, B., Brewer, D., da Rocha, S.R. Propellant-based inhalers for the non-invasive delivery of genes via oral inhalation. *J Control Release* 2012; 157:406-417.
11. Newman SP, Pavia D, Morén F, Sheahan NF, Clarke SW. Deposition of pressurised aerosols in the human respiratory tract. *Thorax* 1981;36:52-55.
12. Vehring R, Foss WR, Lechuga-Ballesteros D. Particle formation in spray drying. *J Aerosol Sci* 2007; 38: 728-746.
13. Chan, H.K., Gonda, I. Development of a systematic theory of suspension inhalation aerosols. II. Aggregates of monodisperse particles nebulized in polydisperse droplets. *Int J Pharm* 1988; 41:147-157.
14. Stein, S.W., Sheth, P., Myrdal, P.B. A model for predicting size distributions delivered from pMDIs with suspended drug *Int J Pharm* 2012; 422:101-115.
15. Chew, N.Y., Chan, H.K. Use of solid corrugated particles to enhance powder aerosol performance. *Pharm Res* 2001; 18, 1570-1577.



16. Louey, M.D., Van Oort, M., Hickey A.J. Aerosol dispersion of respirable particles in narrow size distributions produced by jet-milling and spray-drying techniques. *Pharm Res* 2004; 21:1200-1206.
17. Lastow O, Andersson J, Nilsson A, Balachandran W. Low-voltage electrohydrodynamic (EHD) spray drying of respirable particles. *Pharm Dev Technol* 2007;12:175-181.
18. D.-R. Chen, D.Y.H. Pui, S.L. Kaufman, Electrospraying of conducting liquids for monodisperse aerosol generation in the 4 nm to 1.8  $\mu$ m diameter range. *J Aerosol Sci* 1995; 26:963–977.
19. Deng W, Gomez A. Influence of space charge on the scale-up of multiplexed electrosprays. *J Aerosol Sci* 2007, 38: 1062–1078.
20. Tang K, Gomez A. Monodisperse Electrosprays of Low Electric Conductivity Liquids in the Cone-Jet Mode. *J Colloid Interface Sci* 1996; 184:500-511.
21. Cloupeau M. recipes for use of ehd spraying in cone-jet mode and notes on corona discharge effects. *J Aerosol Sci* 1994; 25 1143-1157.
22. Tang K, Gomez A. Generation by electrospray of monodisperse water droplets for targeted drug delivery by inhalation. *J Aerosol Sci* 1994; 25 1237-1249.
23. Deng W, Klemic JF, Li X, Reed MA, Gomez A. Increase of electrospray throughput using multiplexed microfabricated sources for the scalable generation of monodisperse droplets. *J Aerosol Sci* 2006; 37:696-714.
24. Almekinders JC, Jones C. Multiple jet electrohydrodynamic spraying and applications. *J Aerosol Sci* 1994; 30:969-971.
25. Yang W. Lojewski B, Wei Y, Deng W. Interactions and deposition patterns of multiplexed electrosprays. *J Aerosol Sci* 2012, 46:20-33.
26. Wu WD, Patel KC, Rogers S, Chen XD. Monodisperse Droplet Generators as Potential Atomizers for Spray Drying Technology. *Drying Technology* 2007; 25:1907-1916.
27. Martin G. D., Hoath S. D., Hutchings I. M. Inkjet printing - the physics of manipulating liquid jets and drops. *J Phys Conf Ser* 2008, 105, 1-14 (012001).
28. Berkland C, Kim K, Pack DW. Fabrication of PLG microspheres with precisely controlled and monodisperse size distributions. *J Control Release* 2001; 73:59-74.
29. Berglund RN, Liu BYH. Generation of monodisperse aerosol standards. *Environmental Science & Technology* 1973;7:147-153.
30. Hudd A. Inkjet Printing Technologies. *In The Chemistry of Inkjet Inks*, Magdassi S (Editor) World Scientific Publishing Co Pte Ltd, 2008, pp 3-16.
31. Bogy DB, Talke FE. 'Experimental and theoretical study of wave propagation phenomena in drop-on-demand ink jet devices. *IBM J Res Dev* 1984; 28:314–321.
32. Wijshoff H. The dynamics of the piezo inkjet printhead operation. *Physics Reports* 2010; 491: 77-177.
33. Berger SS., Recktenwald G. Development of an improved model for piezo-electric driven ink jets. *In: Proc. IS&'s NIP19*, 2003, 323-327.
34. Bottiger JR, Deluca PJ, Stuebing EW, Vanreenen DR, An ink jet aerosol generator, *Journal of Aerosol Sci* 1998;29:S965-S966.
35. Patel KC, Chen XD. Production of spherical and uniform-sized particles using a laboratory ink-jet spray dryer. *Asia-Pac J Chem Eng* 2007;2:415–430.
36. Lee E.R. Microdrop Generation. Series Editor: Sergey Edward Lyshevski. CRC Press, 2002.
37. Ehtezazi, T, Horsfield, MA, Barry, PW, O'Callaghan, C. Dynamic change of the upper airway during inhalation via aerosol delivery devices. *J Arosol Med* 2004; 17:325-334.

38. Ehtezazi T, Southern KW, Allanson D, Jenkinson I, O'Callaghan C. Suitability of the upper airway models obtained from MRI studies in simulating drug lung deposition from inhalers. *Pharm Res* 2005; 22:166-170.
39. Kesavan, J., Schepers, DR, Bottiger, JR, King, MD, McFarland, AR. Use of medical metered dose inhalers for functionality testing of bioaerosol detection and identification systems. US Army Research, Development, and Engineering Command, May report. 2012, Available at <http://www.dtic.mil/cgi-bin/GetTRDoc?Location=U2&doc=GetTRDoc.pdf&AD=ADA563525>. Accessed on 5/4/2013.
40. Vervaet, C, Byron, PR. Polystyrene microsphere spray standards based on CFC-free inhaler technology. *J Aerosol Med* 2000, 13:105-115.
41. Adcock IM, Caramori G, Chung KF. New targets for drug development in asthma. *Lancet* 2008; 372(9643):1073-1087.
42. Hirst PH, Pitcairn GR, Weers JG, Tarara TE, Clark AR, Dellamary LA, Hall G, Shorr J, Newman SP. In vivo lung deposition of hollow porous particles from a pressurized metered dose inhaler. *Pharm Res* 2002;19:258-264.
43. Sheng-Chih Shen, Yu-Jen Wang, Yung-Yue Chen. Design and fabrication of medical micro-nebulizer. *Sensors and Actuators A: Physical* 2008;144:135-143.
44. Percin G, Khuri-Yakub BT. Piezoelectrically Actuated Flextensional Micromachined Ultrasound Droplet Ejectors *IEEE Transactions On Ultrasonics, Ferroelectrics, and Frequency Control* 2002;49:756-766.
45. Demirci U, Yaralioglu GG, Hægström E, Percin G, Ergun S, Khuri-Yakub BT. Acoustically actuated flextensional Si<sub>x</sub>N<sub>y</sub> and single-crystal silicon 2-D micromachined ejector arrays. *IEEE Transactions on Semiconductor Manufacturing*. 2004;17:517-524.
46. Rogers S, Fang Y, Lin SXQ, Selomulya C, Chen XD. A monodisperse spray dryer for milk powder: Modelling the formation of insoluble material. *Chem Eng Sci* 2012; 71:75–84.
47. Myrdal PB, Stein SW, Mogalian E, Hoyer W, Gupta A. Comparison of the TSI Model 3306 Impactor Inlet with the Andersen Cascade Impactor: solution metered dose inhalers. *Drug Dev Ind Pharm*. 2004;30:859-868.
48. Mitchell JP, Nagel MW, Avvakoumova V, MacKay H, Ali R. The abbreviated impactor measurement (AIM) concept: part II--Influence of evaporation of a volatile component-evaluation with a "droplet-producing" pressurized metered dose inhaler (pMDI)-based formulation containing ethanol as cosolvent. *AAPS PharmSciTech* 2009;10:252-257.
49. Selvam P, El-Sherbiny IM, Smyth HD. Swellable hydrogel particles for controlled release pulmonary administration using propellant-driven metered dose inhalers. *J Aerosol Med Pulm Drug Deliv* 2011; 24:25-34.
50. Hoe, S., Traini, D., Chan, H.K., Young, P.M. The influence of flow rate on the aerosol deposition profile and electrostatic charge of single and combination metered dose inhalers. *Pharm Res* 2009; 26, 2639-2646.
51. Guidance for Industry, Chemistry, Manufacturing and Controls Documentation for Inhalation, Solution, Suspension and Spray, and Nasal Sprays; Center for Drug Evaluation and Research, Food and Drug Administration, Rockville, MD, 2002.
52. Rathore AS, Winkle H. Quality by design for biopharmaceuticals. *Nat Biotechnol* 2009; 27, 26-34.

**Table 1:** Operational conditions of the inkjet devices to produce droplets.

Powder Formulation	Inkjet Orifice Diameter / $\mu\text{m}$	Feed Solution Concentration (w/v)	Salbutamol Sulphate:PVP Ratio	Peak-to-Peak Voltage/V	Frequency / kHz	Presence of Satellite Droplets
A	1	5%	50:50	20	74	Yes
B	5	0.3%	50:50	22	80	Yes
C	7	0.1%	50:50	8	103	Yes
D	22	0.1%	50:50	20	105	Yes
E	10	0.05%	75:25	22	70	No
F	10	0.05%	50:50	22	125	No
G	14	0.1%	50:50	20	85	No
H	10	0.1%	75:25	22	125	No
I	10	0.3%	75:25	60	10	No

**Table 2:** The Characteristics of the oropharyngeal models.

Subject	Gender	Oral Cavity Inlet Cross Section	Oropharyngeal Opening	Total Volume ( $\text{cm}^3$ )	Oropharyngeal Model Designation	Evaluated Formulation
I	Female	Rectangular	Constricted	37.6	1C	Ventolin
		Circular	Constricted	53.4	2C	Monodisperse
II	Male	Rectangular	Wide	55.9	3A	Ventolin
		Circular	Wide	68.4	4A	Monodisperse
III	Male	Circular	Moderate	75.1	5B	Monodisperse
		Rectangular	Moderate	80.8	6B	Ventolin

**Table 3.** The summary of statistical parameters for primary particle size distributions, and the summary of cascade impaction data, when pMDI formulations were evaluated with the USP induction port.

pMDI Formulation	Primary Particle Diameter/ $\mu\text{m}$ (mean $\pm$ SD)	Primary Particle GSD	Actuator	Spacer	MMAD/ $\mu\text{m}$ (mean $\pm$ SD)	Aerodynamic GSD (mean $\pm$ SD)	%FPF (mean $\pm$ SD)
A	0.65 $\pm$ 0.28	1.60	1	Large	2.20 $\pm$ 0.36	2.08 $\pm$ 0.42	68.94 $\pm$ 6.22
				-	2.30 $\pm$ 0.43	2.92 $\pm$ 0.23	53.95 $\pm$ 4.59
B	1.15 $\pm$ 0.42	1.45	1	Large	2.34 $\pm$ 0.35	1.59 $\pm$ 0.10	64.80 $\pm$ 6.65
C	1.59 $\pm$ 0.38	1.25	1	Large	2.35 $\pm$ 0.43	3.32 $\pm$ 0.37	54.92 $\pm$ 3.83
			2	Small	2.55 $\pm$ 0.37	2.04 $\pm$ 0.49	22.42 $\pm$ 3.77
			1	-	2.56 $\pm$ 0.31	4.71 $\pm$ 0.95	44.43 $\pm$ 8.70
			2	-	3.05 $\pm$ 0.48	2.48 $\pm$ 0.48	21.46 $\pm$ 2.78
D	2.39 $\pm$ 0.68	1.45	1	Large	3.22 $\pm$ 0.50	2.48 $\pm$ 0.70	27.32 $\pm$ 1.70
Ventolin	Not determined		Original	Large	2.40 $\pm$ 0.30	1.74 $\pm$ 0.14	57.32 $\pm$ 1.31
				-	2.56 $\pm$ 0.16	2.16 $\pm$ 0.10	33.48 $\pm$ 1.91
E	1.76 $\pm$ 0.13	1.07	1	Large	2.30 $\pm$ 0.30	1.50 $\pm$ 0.10	69.78 $\pm$ 2.89
F	2.03 $\pm$ 0.43	1.26	1	Large	2.69 $\pm$ 0.68	1.86 $\pm$ 0.37	66.29 $\pm$ 5.46
G	2.36 $\pm$ 0.34	1.14	1	Large	2.05 $\pm$ 0.20	1.63 $\pm$ 0.04	59.18 $\pm$ 12.73
				-	2.00 $\pm$ 0.44	2.36 $\pm$ 0.64	49.31 $\pm$ 8.16
H	2.65 $\pm$ 0.34	1.14	1	Large	3.09 $\pm$ 0.88	1.48 $\pm$ 0.11	46.67 $\pm$ 2.06
I	4.99 $\pm$ 0.28	1.05	1	Large	4.73 $\pm$ 1.68	1.43 $\pm$ 0.10	4.43 $\pm$ 3.99

**Table 4.** Summary of the cascade impaction data when pMDI formulation G (prepared with monodisperse particles) and the Ventolin were evaluated by using the oropharyngeal models.

Oropharyngeal Model	Evaluated Formulation	MMAD/ $\mu\text{m}$ (mean $\pm$ SD)	GSD (mean $\pm$ SD)	%FPF <sup>a</sup> (mean $\pm$ SD)
1C	Ventolin	2.02 $\pm$ 0.96	2.81 $\pm$ 0.26	5.87 $\pm$ 0.81
2C	Monodisperse	2.29 $\pm$ 0.68	1.18 $\pm$ 0.11	3.51 $\pm$ 3.05
3A	Ventolin	2.00 $\pm$ 0.16	2.39 $\pm$ 0.11	14.72 $\pm$ 2.00
4A	Monodisperse	1.66 $\pm$ 0.75	1.28 $\pm$ 0.03	10.43 $\pm$ 0.42
5B	Monodisperse	1.69 $\pm$ 0.22	1.27 $\pm$ 0.05	15.69 $\pm$ 5.51
6B	Ventolin	1.96 $\pm$ 0.18	2.37 $\pm$ 0.19	8.23 $\pm$ 2.25

<sup>a</sup>FPF (percent of the emitted dose that deposited in the impactor).

Figure 1

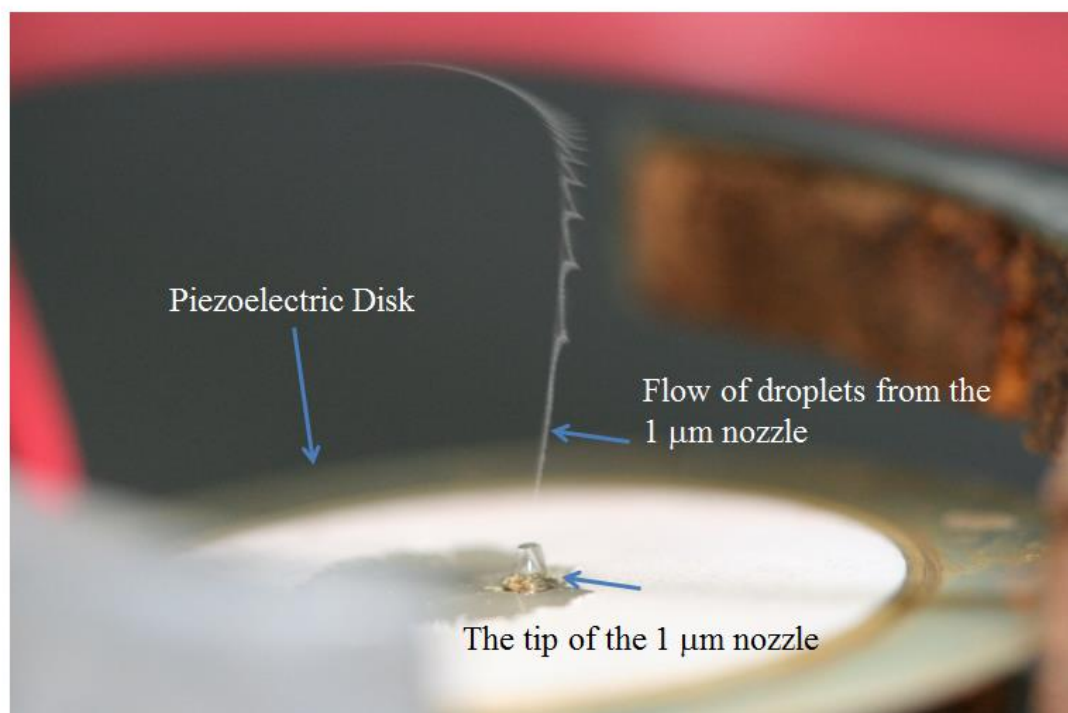


Figure 2

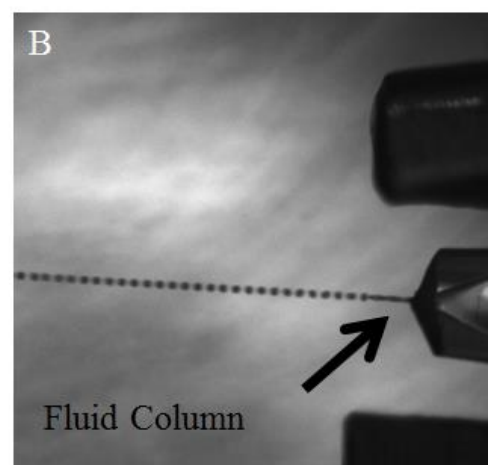
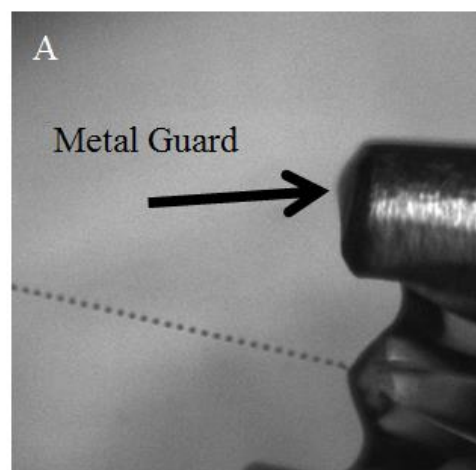


Figure 3

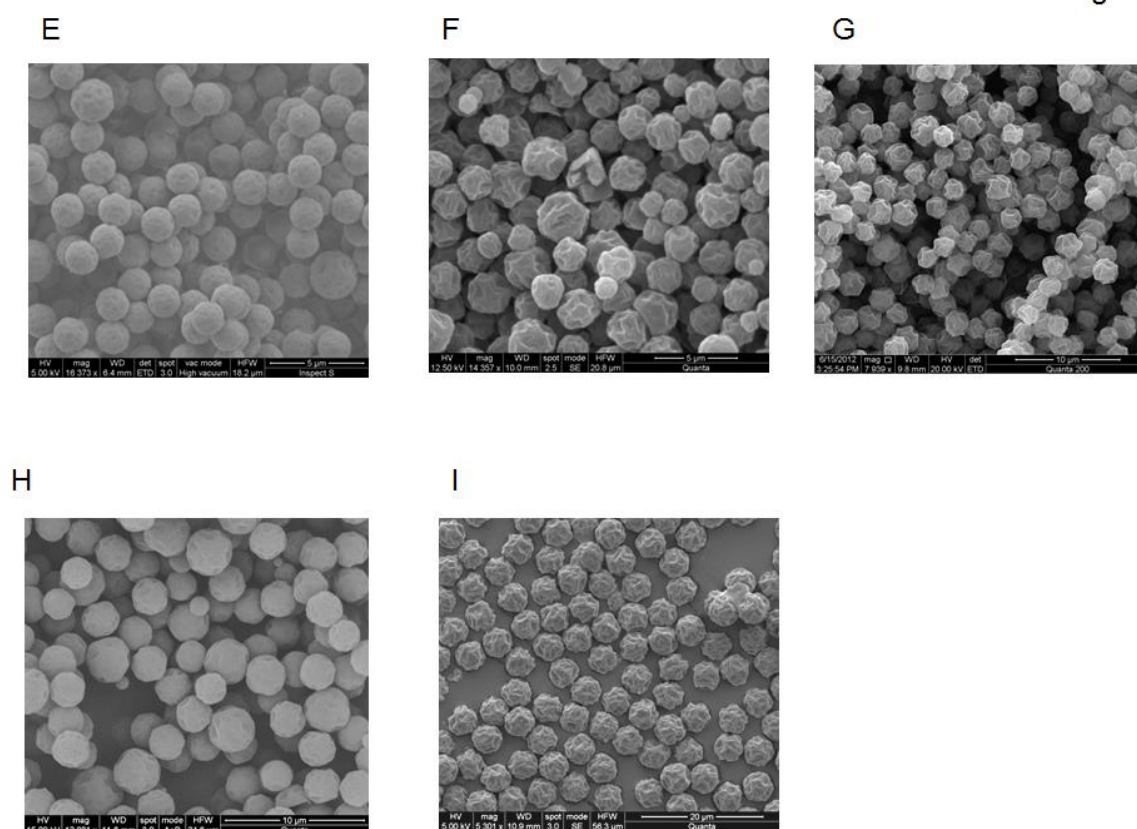






Figure 4A

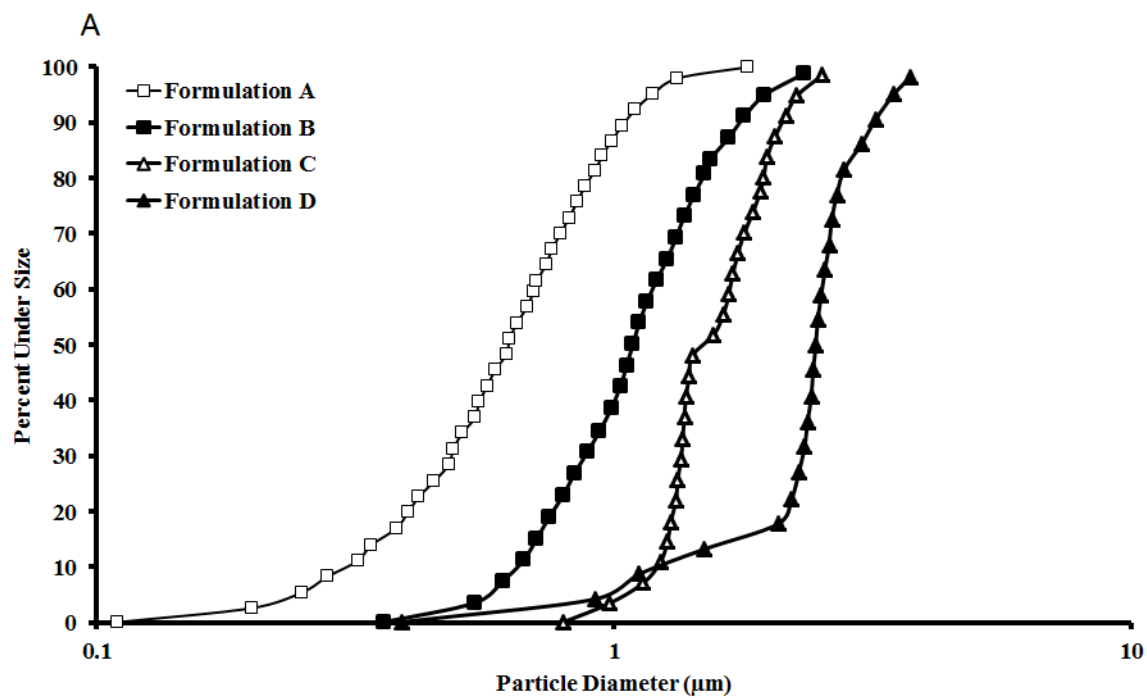


Figure 4B

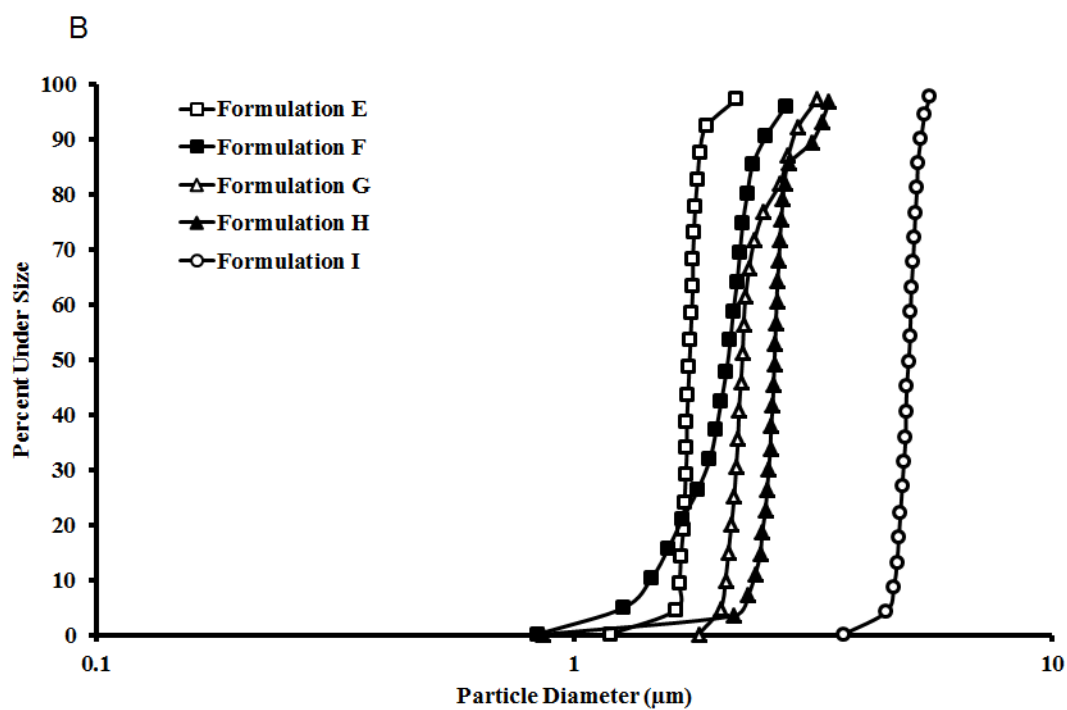


Figure 5

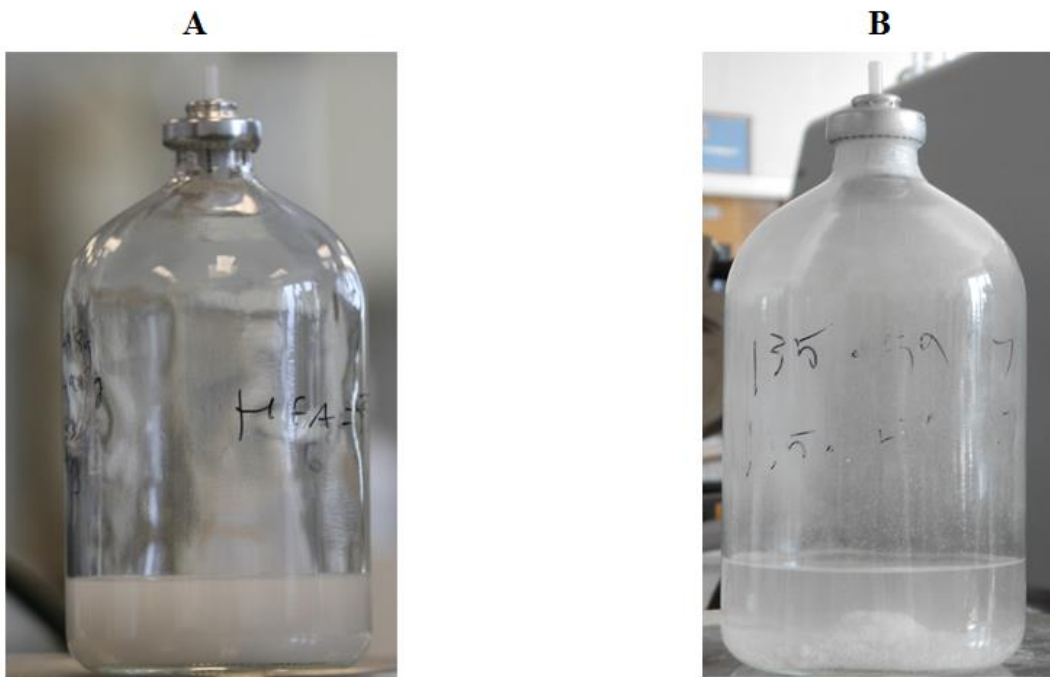


Figure 6A

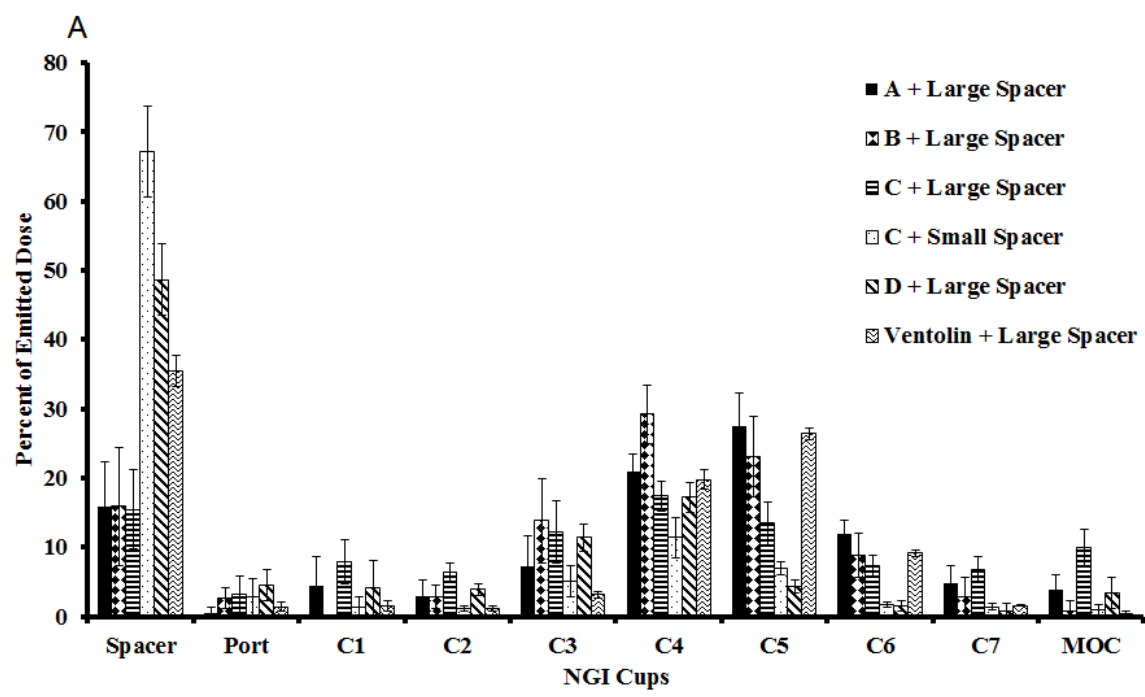


Figure 6B

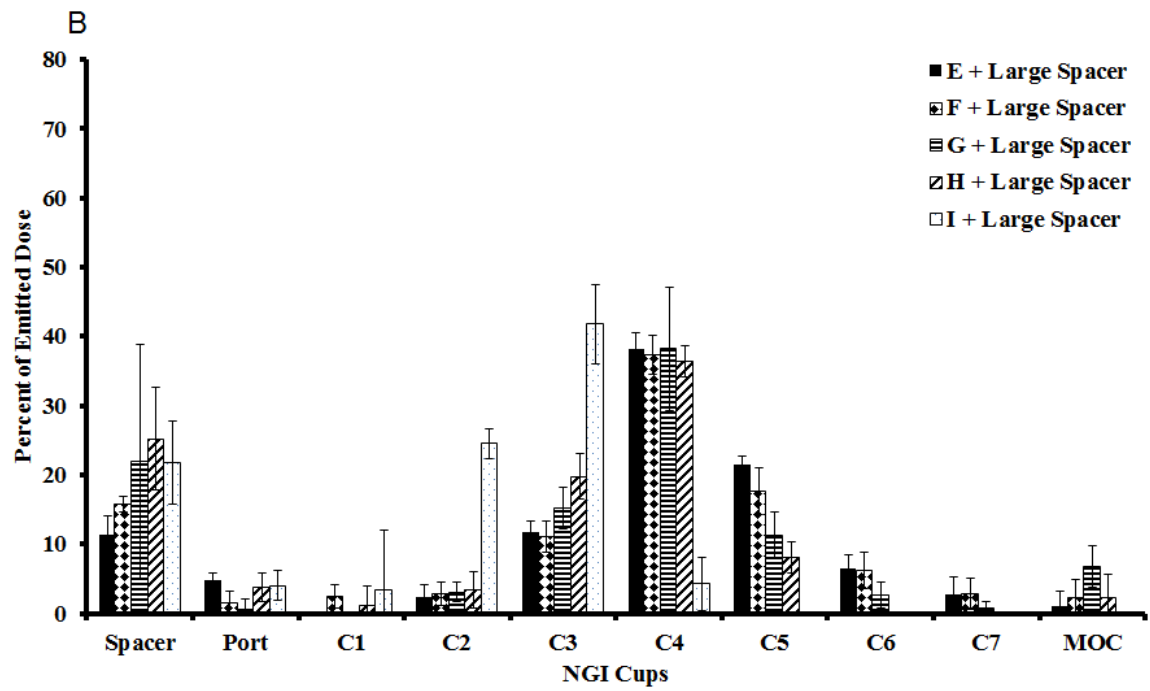


Figure 6C

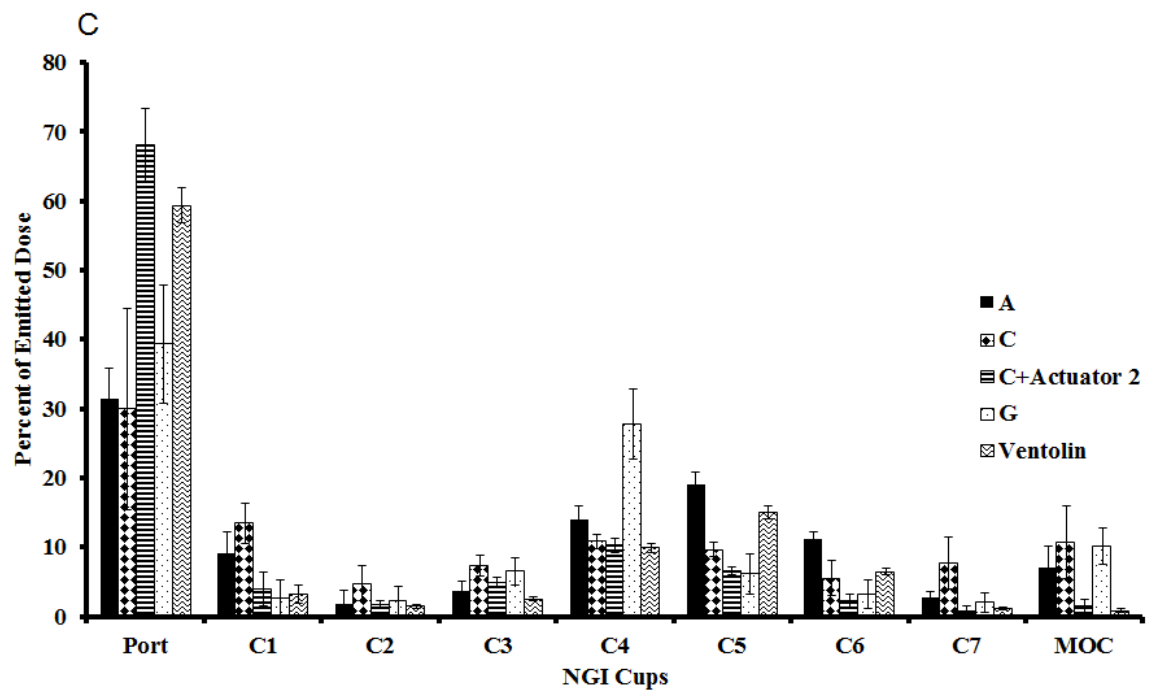


Figure 7A

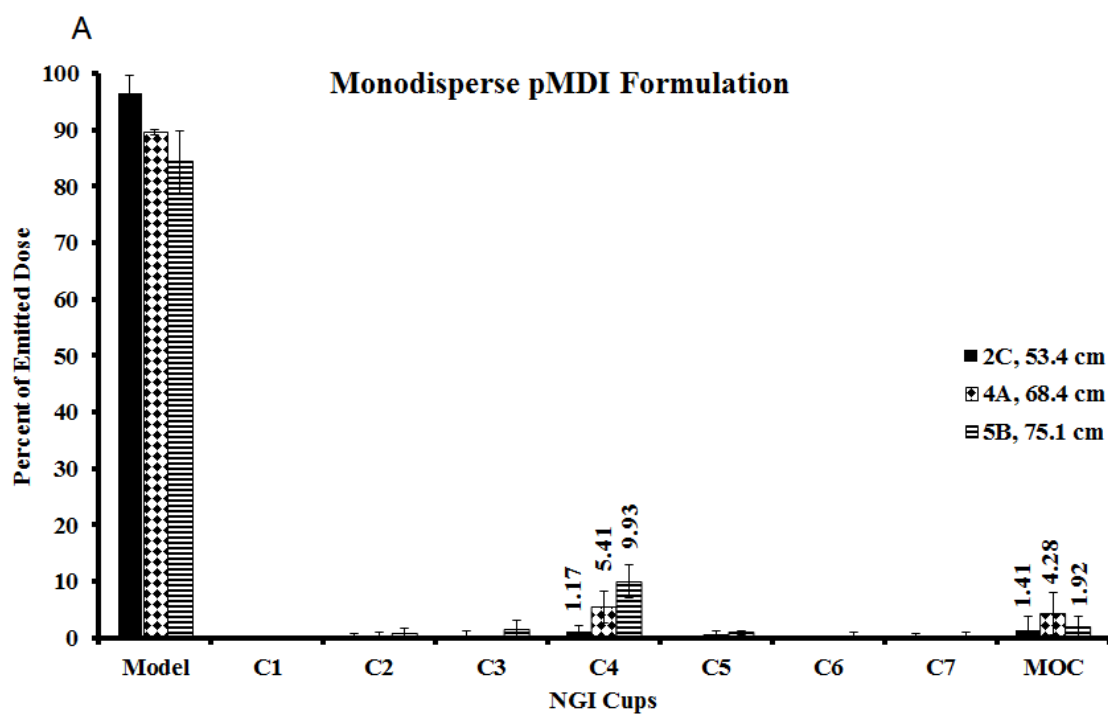


Figure 7B

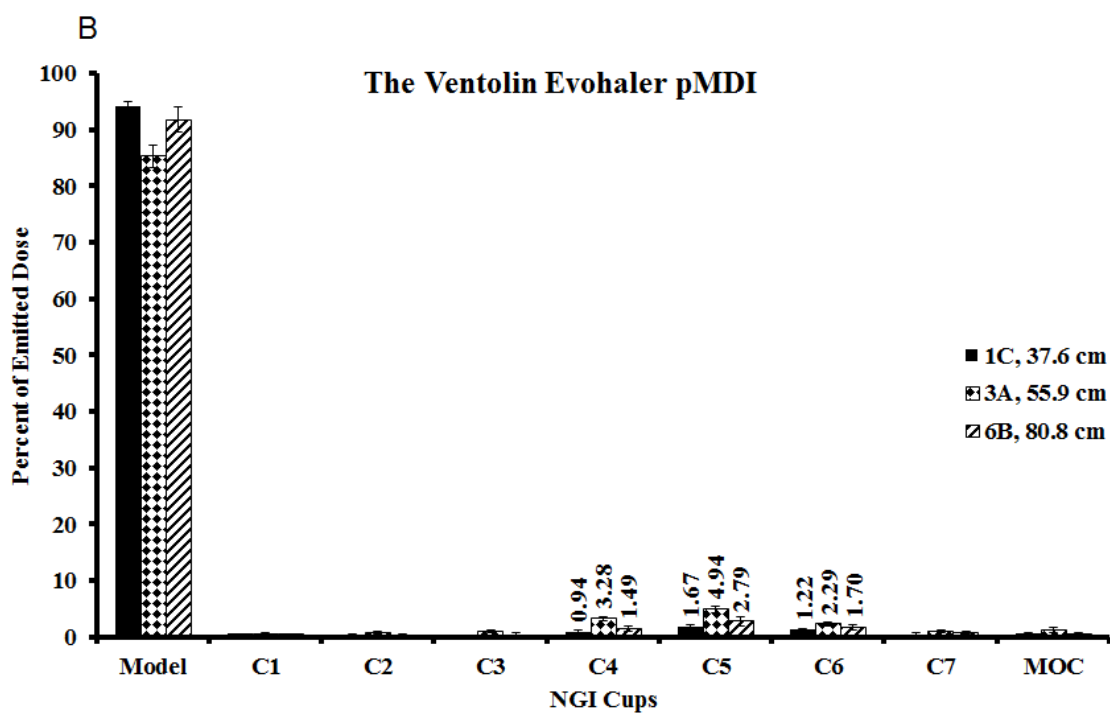
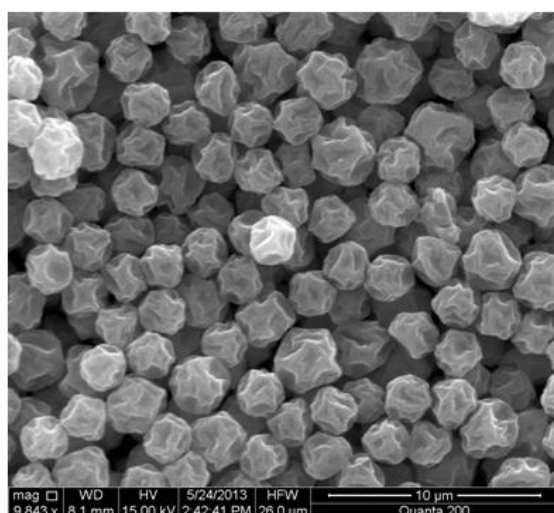
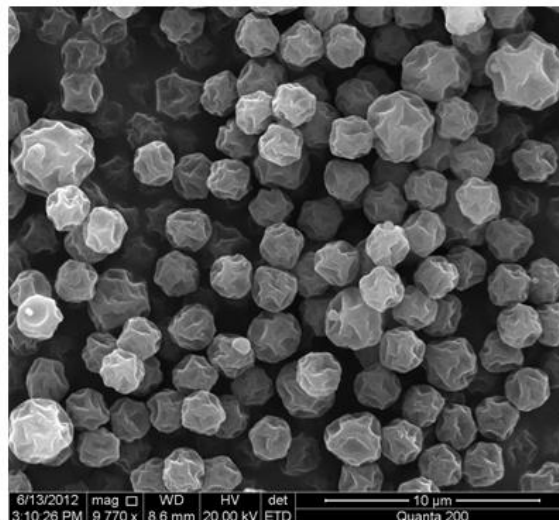


Figure 8



Powder formulation G after  
dispersion in HFA 134a



Powder formulation G prior to  
dispersion in HFA 134a